

## CARI-7A: DEVELOPMENT AND VALIDATION

Kyle Copeland\*

U.S. Federal Aviation Administration, Civil Aerospace Medical Institute, Protection and Survival Research Laboratory, AAM-631, 6500S. MacArthur Blvd, Oklahoma City, OK 73169, USA

\*Corresponding author: kyle.copeland@faa.gov

Received 24 March 2016; revised 31 October 2016; accepted 28 November 2016

Aircrew members can be exposed to higher annual doses of natural ionizing radiation than members of the general population in most parts of the world. The principal ionizing radiation to which they are exposed is galactic cosmic radiation (GCR). Among the particles present in the primary spectrum are heavy ions: relativistic nuclei of lithium and heavier elements. These ions have very high radiation weighting factors and can contribute significantly to the effective dose at altitudes above the Pfofzer maximum. This report describes the latest version of the US Federal Aviation Administration's GCR flight dose calculation software, CARI-7A. Unlike its predecessor, CARI-6, CARI-7A directly includes heavy ion transport, using a database of atmospheric particle spectra generated by incident GCR ions pre-calculated with MCNPX 2.7.0. to enable calculations to the edge of space. Results are compared with measurements aboard commercial passenger aircraft, high altitude research aircraft and similar calculations by others.

## INTRODUCTION

Based on estimates of their exposure from galactic cosmic rays (GCR), solar cosmic rays and radioactive cargo, aircrews of commercial aircraft are among the mostly highly occupationally exposed persons in the world (Table 1)<sup>(1)</sup>. GCR is an ever-present source of exposure, and the most important source for long-term monitoring. The other sources are transient, much less predictable and only rarely exceed GCR intensity during any particular flight.

An increased risk of fatal cancer is the principal health concern associated with exposure to ionizing radiation at the relatively low doses received by crewmembers. There is also evidence of ionizing radiation inducing cataracts in astronauts and miscarriages at unusually low doses<sup>(2, 3)</sup>. Other known effects from ionizing radiation include damage to the central nervous system, and increased risk of cardiovascular disease<sup>(4)</sup>. For the child of a crewmember irradiated during prenatal development, the greatest risks are death *in utero* and fatal cancer. A child is also at risk of inheriting genetic defects because of the radiation received by one or both parents before the child's conception.

At today's commercial flight altitudes, the GCR environment is well characterized for the set of solar activity conditions of the past several decades<sup>(5–8)</sup>. There are many models to choose among that give a fairly accurate assessment of doses accumulated over a career of flying, some of them are based entirely on fits to available survey data<sup>(9)</sup>. However, these tools are inadequate for the new era of flight that approaches. Suborbital commercial flights could begin on a regular basis within a few years, and multi-hour balloon flights

at 30 km ( $11 \text{ g cm}^{-2}$ ) are already offered to those seeking to view the blackness of space and curvature of the Earth<sup>(10)</sup>. While suborbital rocket-plane flights will reach greater altitudes, the balloon flights offer significant time at altitudes well above the limits of most existing models.

The difficulty of extreme altitude GCR dosimetry comes from the presence of fully ionized lithium and other heavier nuclei in the primary GCR spectrum. Primary nuclides up to and including iron are considered potentially important sources of biological dose in interplanetary space<sup>(11)</sup>. Lei *et al.* calculate that while protons would contribute almost 60% of the absorbed dose to a spacecraft occupant from GCR behind a shield of  $1 \text{ g cm}^{-2}$  polyethylene, protons would contribute only about 20% of the dose equivalent. In terms of health effects in high-altitude aircraft and spacecraft crewmembers resulting from exposure to these particles, these are among the least understood particles present in the GCR spectrum. Collectively, they most often are referred to as HZE (high nuclear charge,  $Z$ , and energy,  $E$ ) particles or sometimes as *metals* (the more common name in astronomy). These atomic nuclei traveling at relativistic speeds produce ionization tracks of extreme density, resulting in unique biological damage that is still poorly understood. In the past, they were often converted into constituent nucleons prior to transport in atmospheric transport calculations (called the *superposition approximation*) to simplify the transport problem. This resulted in increasingly inaccurate calculations for altitudes above the Pfofzer maximum (almost all HZE flux is already broken into lighter nuclear fragments or nucleons before reaching this altitude).

**Table 1. Ten highest average annual effective doses among monitored workers worldwide (1990–94)<sup>(1)</sup>.**

Practice	Rank	Effective dose, mSv y <sup>-1</sup>
Above-ground radon from oil and natural gas extraction	1	4.8
Nuclear fuel mining	2	4.5
Nuclear fuel milling	3	3.3
Aircrew	4	3.0
Mining other than nuclear fuel or coal	5	2.7
Radioisotope production	6	1.93
Industrial radiography	7	1.58
Nuclear fuel reprocessing	8	1.5
Reactor operation	9	1.4
Nuclear fuel fabrication	10	1.03

CARI-7A was developed to overcome several limitations of CARI-6: the altitude limit for calculations has been extended from 27 to 100 km; the superposition approximation is now an option, not a requirement; a Disc Operating System (DOS) emulator is not needed on modern systems; the user can now choose from multiple GCR models; Forbush decreases and geomagnetic storm effects are now included directly; particle flux, modern effective dose and ambient dose equivalent ( $H^*(10)$ ) dose outputs are new options<sup>(12, 13)</sup>.

## METHODS

### Overview

CARI-7A extends to GCR particle spectra the methods of calculation of solar energetic particle dose rates used in Copeland *et al.*, using an updated transport code<sup>(14)</sup>. It uses modern GCR models, combined with atmospheric shower data calculated using the well proven Monte Carlo particle transport software MCNPX 2.7.0, which is capable of modeling high energy nuclear interactions of HZE with atmospheric atoms<sup>(15, 16)</sup>. This makes use of the superposition approximation unnecessary. To build CARI-7A, MCNPX 2.7.0 was used to calculate a database of atmospheric particle spectra resulting from isotropically incident primary GCR particles with energies up to 1 TeV at selected altitudes. The particle spectra at each altitude were then converted to doses using published sets of fluence-to-dose conversion coefficients. With these base data, the atmospheric response to the incident GCR fluence could be scaled to match the GCR fluence for any past or future conditions. The resulting model was then compared with measurements and with other models capable of like calculations. To the extent possible, comparisons were made at both commercial flight

altitudes and altitudes above the Pfotzer maximum. At lower altitudes this included many of the most well-known flight dose calculator programs, while at higher altitudes results from NAIRAS and PHITS were used<sup>(17, 18)</sup>. A basic description follows. Variations from the description of CARI-7 in the work of Copeland<sup>(12)</sup> indicate recent modifications.

### GCR Models

There are multiple models available to provide the GCR environment at the top of the atmosphere. Based on a NASA evaluation of GCR models, two are currently included in CARI-7A: the ISO 15390:2004 (ISO) model and the Badhwar and O'Neill 2011 (BO11) model<sup>(19–21)</sup>. The ISO and BO11 models are two of the best modern models available. Each of these models provides the GCR spectrum at Earth's orbit (i.e. at a distance of 1 AU from the Sun), but away from Earth's magnetic field, by means of solar modulation of an assumed constant local interstellar GCR spectrum (LIS). As incorporated, each model retains its own LIS and solar modulation. These models can readily be replaced or new models added with little or no (in the case of a pre-calculated custom spectrum) coding effort.

To account for Forbush decreases and other minor variations in solar activity on the scale of an hour to a day from transient space weather, flux is modulated in direct proportion (1:1) to hourly changes in neutron monitor count rate fluctuations at a high-latitude, near-sea-level monitor, as proposed by Lantos<sup>(22)</sup>. For times prior to October 1995, after which it was shut down, Deep River neutron monitor data are used. From then to present, data from the Apatity neutron monitor are used.

### Particles

While it varies with solar activity, the interplanetary cosmic radiation consists of about 85% protons, 14%  $\alpha$ -particles and 1% heavier nuclei, and fluxes for elements heavier than iron are orders of magnitude less than iron<sup>(23)</sup>. Primary GCR chosen for transport (H-Fe ions for nuclear transport, equivalent p and n fluxes for the superposition approximation) were selected on the basis of expected importance to the dose rates in the atmosphere. In addition to these ions, other particles transported were: neutrinos, kaons, muons, pions, photons,  $e^+$ ,  $e^-$ , n,  $d^+$ ,  $t^+$  and  $^3\text{He}^{++}$ . Kaons, neutrinos and  $\pi^0$  were not included in dose tallies.

### Geomagnetism

MCNPX 2.7.0 does not allow the definition of external magnetic fields, so field effects are included as modulations to the primary GCR input spectrum at

the top of the atmosphere using effective vertical cutoff rigidity ( $R_V$ ) grids as the basic data to generate high-pass filters for access to the atmosphere at the user entered location and altitude<sup>(24–29)</sup>. Al Anid's method is used to adjust the effective vertical cutoff rigidity during geomagnetic disturbances having a Kp index greater than 5 (i.e. geomagnetic storms)<sup>(30)</sup>.

Once the effective vertical cutoff is calculated, the sky above the horizon at the target location and altitude is divided into 900  $\sim 1.9^\circ$  by  $20^\circ$  sectors based on average zenith and azimuth angles (roughly the minimum needed to stabilize the numerical integration when including zenith and azimuth related effects). Two options are available to the user for handling the cutoff rigidities during atmospheric transport.

For the first option,  $R_V$  is assigned to all sectors, i.e.  $R_V$  is used as the cutoff rigidity for the whole sky. In this approach, particles entering the atmosphere from any direction with rigidity below  $R_V$  are rejected. Clem *et al.* used the Monte Carlo radiation transport code FLUKA coupled to their neutron monitor response functions, to estimate the accuracy of this approximation for locations of measurements at sea level during their 1994–95 ship-born latitude survey<sup>(31, 32)</sup>. They found the vertical cutoff to be within 10% of apparent cutoff from 2 to 13 GV, with the accuracy improving (in terms of per cent difference) at larger cutoffs. Analysis by Dorman *et al.* of a more recent (1996–97) and extensive ( $\sim 1$ –17 GV) Italian ship-born latitude survey confirmed the earlier findings<sup>(33)</sup>.

The second option uses the method of Smart and Shea, based on Störmer's equation, to calculate non-vertical cutoffs,

$$R_\alpha = 4R_V \left\{ \left[ 1 + (1 - \sin(\epsilon) \sin(\phi) \cos^3(\lambda))^{1/2} \right]^2 \right\}^{-1}, \quad (1)$$

where  $R_\alpha$  is the cutoff rigidity in angular direction  $\alpha$ ,  $\epsilon$  the angle from zenith,  $\phi$  the azimuthal angle measured clockwise from magnetic north and  $\lambda$  is the geomagnetic latitude<sup>(34, 35)</sup>.

### GCR in Earth's Atmosphere

The model atmosphere used was a 100 km deep version of the 1976 US Standard Atmosphere adapted for use in MCNPX<sup>(14, 36)</sup>. It consists of a single profile representing the idealized, steady-state atmosphere for moderate solar activity.

MCNPX 2.7.0 was used to calculate the atmospheric particle fluence spectra per unit primary particle fluence resulting from GCR ions interacting with the atmospheric constituents. Primaries entered

the model atmosphere isotropically at 100 km altitude with energies from 1 MeV to 1 TeV, at  $1\times$ ,  $2\times$ , and  $5\times$  for each order of magnitude. This was considered fine enough to minimize computation time while still providing some detail of variations within each power of ten. Because charged nuclei with energies below 1 MeV are quickly stopped (e.g. a 1 MeV He-4 ion has a range of about 0.6 cm in dry air at STP), 1 MeV was chosen as the minimum energy for primary GCR ions<sup>(37)</sup>. The upper limit of 1 TeV was adopted based on discussions with MCNPX developers<sup>(38)</sup>. Reasons for this included: photon and electron models go out of range at 50 GeV and begin extrapolating; particles not transported deposit their energies locally in MCNPX and proton and neutron transport is not verified at energies beyond 1 TeV.

When treating the MCNPX calculated shower data as beam-like in CARI, as an alternative treatment of the angle-dependent cutoff rigidities, a zenith-dependent slant function approximating a Chapman function is included:

$$X_{\text{NonVertical}} = X (\cos(\epsilon))^{-1}, \quad (2)$$

where  $X$  is the vertical depth in  $\text{g cm}^{-2}$  and  $\epsilon$  is again the angle from zenith in radians<sup>(39)</sup>. A radiation length of  $132 \text{ g cm}^{-2}$  is used when extrapolating results to slant depths exceeding  $1035 \text{ g cm}^{-2}$ , the maximum depth of calculated isotropic shower data<sup>(40)</sup>.

### Options

CARI-7A offers the user four options for transport of atmospheric showers:

- (1) Use  $R_V$  as the cutoff rigidity for all angles of approach and use the isotropic shower data as is (as was done with SPE protons and alphas in the work of Copeland *et al.*<sup>(14)</sup>).
- (2) Treat the isotropically incident shower as is, and use angle-dependent cutoff rigidities to limit isotropic shower entry using Equation (1).
- (3) Use  $R_V$  as the cutoff rigidity for all angles of approach, and treat the isotropically incident shower data as if it were beam-like, using slant depths calculated with Equation (2).
- (4) Treat shower data as beam-like, use both angle-dependent cutoff rigidities and slant depths.

For each of the four transport options, showers may be constructed using either the full set of nuclear transport shower data (i.e. protons through iron nuclei enter the atmosphere, referred to as nuclear transport below) or with superposition approximation treatment of the shower data (after geomagnetic filtering, alphas and heavier ions enter the atmosphere as equivalent added fluences of free neutrons and protons of the same energy per nucleon).

## Fluence to Dose Conversion

Five output options are available: atmospheric particle fluence, effective dose based on ICRP Pub. 60 recommendations ( $E_{60}$ ), effective dose based on ICRP Pub. 103 recommendations ( $E_{103}$ ), ambient dose equivalent  $H^*(10)$ , and whole-body absorbed dose<sup>(41–43)</sup>. For any of the doses, either the total or the dose from a specific particle can be calculated (a complete list of 37 particles is in the work of Copeland<sup>(12)</sup>).

While close to the Earth, isotropic-from-above exposure models are more realistic than isotropic models of vehicle occupant irradiation<sup>(44)</sup>. However, sufficiently large sets of fluence-to-dose conversion coefficients to be useful for aviation cosmic ray dosimetry only exist for isotropic, posterior–anterior and anterior–posterior exposures (for isotropic irradiation imagine being at the center of a radioactive sphere, the radiation is the same from all directions, isotropic-from-above irradiation is analogous to being inside a radioactive dome with a radiation absorbent floor)<sup>(45–51)</sup>. CARI-7A uses isotropic exposure coefficients, since these provided the best match to the isotropic-from-above exposure coefficients where matching coefficients could be compared. For particles where coefficients for  $H^*(10)$  are unavailable, coefficients for  $E_{103}$  are directly used as substitutes. For particle energies outside the range in the tables, values at the extremes are used.

## Flight Doses

Flight doses are calculated by integrating single location doses along the flight path calculated from the user input flight data. It is assumed that the flight follows a flight path described by a geodesic (i.e. the shortest possible route) between origin and destination airports and starts at the beginning of the hour specified (if any). The geodesic route information is calculated using the programs FORWARD and INVERSE<sup>(52)</sup>. In calculation of the flight path, a constant speed is assumed, as are constant rates of climb and descent. Output is calculated for each minute of the flight and summed for the total.

## Program Uncertainties

In the sense that CARI-7A treats MCNPX shower data, the GCR models and the fluence-to-dose conversion coefficients as constants, results are deterministic, i.e. they are always the same for the same calculation. The reported uncertainties are only statistical and analogous to the uncertainties reported with the fluence-to-dose coefficients calculated with FLUKA and particle fluence uncertainties reported by MCNPX<sup>(12, 15, 16, 44, 45)</sup>. They are the accumulated

statistical uncertainty of the results in terms of the calculation process. When combined assuming independence and normality, these vary with altitude and vertical cutoff rigidity, coming to about 0.5% (0.1–0.8%) for effective dose (to the degree the data are not truly independent, etc., this is underestimated). The low statistical uncertainty in the shower data is the result of over five million core-hours of simulations on the High-Performance Aerospace Medical Research Computing System (HiPARCoS) cluster at the US Federal Aviation Administration's Civil Aerospace Medical Institute in OK City, OK and Compute Canada's High Performance Computing Virtual Laboratory (HPCVL).

There are several other sources of uncertainty in the models which are larger than this, including known weaknesses in the methods, such as: the lack of local magnetic field effects in MCNPX with regards to particle paths; disregard of re-entrant particles; GCR model differences (evident from comparison of ISO and BO11 results included below); approximations used to assign unknown fluence-to-dose conversion coefficients, such as the heavy ion coefficients; the assignment of effective vertical cutoff rigidities; effect of aircraft structure and loading and the atmosphere model<sup>(12, 31, 33, 34, 53–56)</sup>. Combining the estimated uncertainties from these sources and a safety factor of 2 for a single point calculation at  $250 \text{ g cm}^{-2}$  resulted in an estimated uncertainty of 33%.

## RESULTS AND VERIFICATION

### Results

Tables 2–5 show calculated altitude profiles for effective dose,  $E_{103}$ , for conditions of ICRU solar minimum and solar maximum at both near the geomagnetic equator and at polar latitude, calculated using the two GCR models and nuclear transport, both with and without angle-dependent cutoffs and slant depths. Results calculated using the ISO GCR model are very similar to those calculated using the BO11 GCR model, but consistently higher at  $R_v = 17 \text{ GV}$ .

The results calculated using the zenith and azimuth dependent options indicate the non-vertical cutoff effect is weak, suggesting a maximum reduction of about 4%. Of course, because the shower data at each depth going into the dose calculations were not generated originally from beams of primaries but from primaries leaving the whole top of the atmosphere isotropically, using the data in this beam-like way is an approximation. Excessive attenuation is expected at great depths, and indeed, while differences are slight at low depths, near sea level the doses are close to a factor of three lower.

**Table 2. Effective dose rates at selected altitudes calculated for the ICRU 1998 solar minimum using the BO11 GCR model and nuclear transport.**

Depth/Option <sup>a</sup>	Vertical cutoff rigidity = 0 GV				Vertical cutoff rigidity = 17 GV			
	1	2	3	4	1	2	3	4
1000	0.0716	0.0716	0.0237	0.0237	0.0580	0.0569	0.0194	0.0190
900	0.112	0.112	0.0379	0.0379	0.0805	0.0788	0.0293	0.0287
700	0.337	0.337	0.119	0.119	0.191	0.187	0.0736	0.0720
500	1.17	1.17	0.483	0.483	0.558	0.546	0.241	0.236
300	3.69	3.69	2.84	2.84	1.45	1.42	1.14	1.12
200	7.22	7.22	3.98	3.98	2.27	2.22	1.35	1.33
125	11.7	11.7	7.32	7.32	2.83	2.77	2.01	1.97
85	14.7	14.7	8.51	8.51	2.93	2.87	1.98	1.94
70	17.4	17.4	10.8	10.8	2.94	2.89	2.20	2.17
50	23.2	23.2	15.6	15.6	3.18	3.13	2.62	2.58
30	27.1	27.1	19.0	19.0	3.31	3.26	2.83	2.79
20	31.6	31.6	22.1	22.1	3.47	3.43	2.91	2.87
15	39.8	39.8	36.1	36.1	3.77	3.74	3.64	3.60
10	45.8	45.8	34.0	34.0	4.03	4.01	3.53	3.50
5	52.1	52.1	41.6	41.6	4.25	4.23	3.83	3.80
2	67.0	67.0	55.1	55.1	4.99	4.98	4.48	4.46
1	77.9	77.9	65.7	65.7	5.44	5.43	4.87	4.86

<sup>a</sup>Options: (1) isotropic showers,  $R_\alpha = R_V$ ; (2) isotropic showers,  $R_\alpha$  from Equation (1); (3) shower data treated as beams using Equation (2),  $R_\alpha = R_V$  and (4) shower data treated as beams using Equation (2),  $R_\alpha$  from Equation (1).

**Table 3. Effective dose rates at selected altitudes calculated for the ICRU 1998 solar minimum using the ISO GCR model and nuclear transport.**

Depth/Option <sup>a</sup>	Vertical Cutoff rigidity = 0 GV				Vertical cutoff rigidity = 17 GV			
	1	2	3	4	1	2	3	4
1000	0.0815	0.0815	0.0270	0.0270	0.0678	0.0667	0.0227	0.0223
900	0.126	0.126	0.0429	0.0429	0.0937	0.0920	0.0342	0.0336
700	0.369	0.369	0.132	0.132	0.221	0.216	0.0853	0.0837
500	1.26	1.26	0.523	0.523	0.644	0.632	0.279	0.273
300	3.93	3.93	3.03	3.03	1.67	1.64	1.31	1.29
200	7.60	7.60	4.20	4.20	2.58	2.54	1.55	1.52
125	12.1	12.1	7.64	7.64	3.19	3.13	2.28	2.23
85	15.0	15.0	8.79	8.79	3.29	3.24	2.23	2.19
70	17.6	17.6	11.1	11.1	3.30	3.24	2.48	2.45
50	23.0	23.0	15.7	15.7	3.56	3.50	2.95	2.90
30	26.4	26.4	18.8	18.8	3.72	3.66	3.19	3.13
20	30.4	30.4	21.6	21.6	3.91	3.85	3.28	3.23
15	37.4	37.4	34.2	34.2	4.28	4.23	4.12	4.07
10	42.6	42.6	32.2	32.2	4.60	4.55	4.00	3.96
5	47.9	47.9	38.9	38.9	4.88	4.83	4.36	4.31
2	60.9	60.9	50.6	50.6	5.77	5.73	5.15	5.10
1	70.5	70.5	59.8	59.8	6.34	6.29	5.65	5.60

<sup>a</sup>Options: (1) isotropic showers,  $R_\alpha = R_V$ ; (2) isotropic showers,  $R_\alpha$  from Equation (1); (3) shower data treated as beams using Equation (2),  $R_\alpha = R_V$  and (4) shower data treated as beams using Equation (2),  $R_\alpha$  from Equation (1).

### Comparison with Measurements

Most of the calculations shown in this section used the BO11 GCR model and nuclear transport. Reasoning for these choices was (1) the BO11 model

is believed to be the more accurate of the two GCR models<sup>(21)</sup>; (2) while non-vertical magnetic cutoffs have been found by Felsberger *et al.* to be important at low latitude and altitude using PLOTINUS,

**Table 4. Effective dose rates at selected altitudes calculated for the ICRU 2002 solar maximum using the BO11 GCR model and nuclear transport.**

Depth/Option <sup>a</sup>	Vertical cutoff rigidity = 0 GV				Vertical cutoff rigidity = 17 GV			
	1	2	3	4	1	2	3	4
1000	0.0669	0.0669	0.0222	0.0222	0.0567	0.0556	0.0190	0.0186
900	0.102	0.102	0.0350	0.0350	0.0783	0.0767	0.0286	0.0280
700	0.290	0.290	0.105	0.105	0.185	0.181	0.0714	0.0698
500	0.969	0.969	0.404	0.404	0.539	0.527	0.233	0.228
300	3.18	3.18	1.61	1.61	1.46	1.43	0.782	0.766
200	5.47	5.47	3.06	3.06	2.17	2.13	1.30	1.27
125	8.45	8.45	5.40	5.40	2.69	2.63	1.92	1.88
85	10.2	10.2	6.07	6.07	2.78	2.72	1.89	1.84
70	11.8	11.8	8.06	8.06	2.86	2.80	2.31	2.26
50	15.1	15.1	10.4	10.4	2.99	2.93	2.48	2.43
30	19.8	19.8	14.2	14.2	3.24	3.18	2.73	2.68
20	24.1	24.1	22.1	22.1	3.52	3.46	3.39	3.34
15	27.4	27.4	20.9	20.9	3.75	3.70	3.30	3.25
10	30.7	30.7	25.0	25.0	3.94	3.90	3.57	3.52
5	38.6	38.6	32.3	32.3	4.62	4.57	4.16	4.11
2	43.9	43.9	37.6	37.6	5.03	4.98	4.51	4.46
1	46.8	46.8	43.7	43.7	5.29	5.24	5.04	4.99

<sup>a</sup>Options: (1) isotropic showers,  $R_\alpha = R_V$ ; (2) isotropic showers,  $R_\alpha$  from Equation (1); (3) shower data treated as beams using Equation (2),  $R_\alpha = R_V$  and (4) shower data treated as beams using Equation (2),  $R_\alpha$  from Equation (1).

**Table 5. Effective dose rates at selected altitudes calculated for the ICRU 2002 solar maximum using the ISO GCR model and nuclear transport.**

Depth/Option <sup>a</sup>	Vertical cutoff rigidity = 0 GV				Vertical cutoff rigidity = 17 GV			
	1	2	3	4	1	2	3	4
1000	0.0779	0.0779	0.0259	0.0259	0.0671	0.0660	0.0225	0.0221
900	0.117	0.117	0.0406	0.0406	0.0926	0.0909	0.0338	0.0333
700	0.330	0.330	0.119	0.119	0.218	0.213	0.0842	0.0825
500	1.09	1.09	0.46	0.46	0.634	0.621	0.274	0.269
300	3.58	3.58	1.81	1.81	1.71	1.68	0.917	0.899
200	6.14	6.14	3.44	3.44	2.53	2.48	1.52	1.49
125	9.45	9.45	6.05	6.05	3.12	3.06	2.23	2.18
85	11.3	11.3	6.79	6.79	3.22	3.15	2.19	2.14
70	13.2	13.2	9.00	9.00	3.31	3.24	2.67	2.62
50	16.7	16.7	11.6	11.6	3.46	3.40	2.88	2.82
30	21.6	21.6	15.6	15.6	3.79	3.72	3.19	3.13
20	26.1	26.1	24.0	24.0	4.15	4.08	4.00	3.93
15	29.6	29.6	22.7	22.7	4.46	4.39	3.89	3.82
10	32.9	32.9	27.0	27.0	4.73	4.66	4.23	4.16
5	41.2	41.2	34.6	34.6	5.60	5.52	4.99	4.92
2	46.8	46.8	40.1	40.1	6.14	6.06	5.47	5.40
1	49.9	49.9	46.6	46.6	6.48	6.39	6.15	6.06

<sup>a</sup>Options: (1) isotropic showers,  $R_\alpha = R_V$ ; (2) isotropic showers,  $R_\alpha$  from Equation (1); (3) shower data treated as beams using Equation (2),  $R_\alpha = R_V$  and (4) shower data treated as beams using Equation (2),  $R_\alpha$  from Equation (1).

results in Tables 2–5 indicate that for the methods used here the effect was weak<sup>(57)</sup>; (3) the shower data are from simulated isotropic irradiation of the whole sky; and (4) nuclear transport is more realistic than the superposition approximation at high altitudes<sup>(58)</sup>.

#### Measurements at high altitudes

High-altitude ER-2 airplane flights were part of the Atmospheric Ionizing Radiation 2 (AIR-2) research campaign in support of high-speed civilian transport

aircraft development in the late 1990s<sup>(59, 60)</sup>. For these flights several instruments were mounted inside the ER-2, and the airplane flew mostly at altitudes near 20 km. In Figure 1, CARI-7A calculations using both the GCR models (ISO and BO11) with angle-dependent cutoff rigidities and non-vertical depths, and nuclear transport are shown with TEPC data from the AIR-2 North-South flights. The dip in dose equivalent rate values at cutoff rigidities near 0 GV is the result of mid-flight descents to make lower-altitude measurements at that cutoff. The dip in dose equivalent rate at cutoff rigidity near 5 GV is because the airplane was close to its origin airport at cutoff rigidity 4.4 GV and had not yet reached cruising altitude or just started final descent.

In Table 6, total neutron flux results calculated using multiple options are shown, along with the neutron flux measurements made during the AIR-2 campaign<sup>(53, 61, 62)</sup>. Calculations without using any

angular dependencies are very good, even with superposition, while the fully beam-like use of the data results in increasingly too much attenuation with increasing depth.

Table 7 shows whole-body absorbed dose calculations (using the BO11 GCR model, angular cutoffs, depth related corrections and nuclear transport) compared with High Altitude Radiation Environment Study (HARES) data from May and June 1971 collected with a 20-cm diameter tissue equivalent LET spectrometer developed at Brookhaven National Laboratory<sup>(63, 64)</sup>. These measurements were part of a joint program by NASA, FAA and USAF to measure dose rates commercial and supersonic transport cruise altitudes and were estimated to be 15–20% uncertain at the 90% confidence level considering counting statistics, estimated calibration and amplifier setting errors, and temperature effects. Agreement is excellent.

#### Measurements at commercial flight altitudes

In 2010 the ICRU published a set of  $H^*(10)$  values derived from measurements for commercial flight altitudes at depths of 293, 243 and 201 g cm<sup>-2</sup> (flight

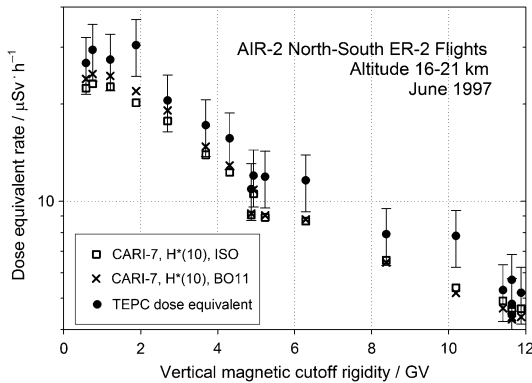


Figure 1. TEPC measurements of dose equivalent rate from the June 1997 North-South ER-2 flights of NASA's AIR-2 flight campaign compared with CARI-7A calculations of  $H^*(10)$ <sup>(59, 60)</sup>. Error bars shown are for TEPC measurements. In each case, model calculations used angle-independent calculations and nuclear transport.

Table 7. Comparison of absorbed dose calculations with May and June 1971 HARES flight data<sup>(63, 64)</sup>.

Flight level	CARI-7 A $\mu\text{Gy h}^{-1}$	HARES <sup>a</sup> $\mu\text{Gy h}^{-1}$	CARI-7A % deviation from HARES
300	1.79	1.59( $\pm 0.31$ )	12.6
380	2.93	2.88( $\pm 0.58$ )	1.7
500	4.41	4.89( $\pm 0.98$ )	-9.8
600	5.23	6.03( $\pm 1.21$ )	-13.3

<sup>a</sup>Data are reported with 90% confidence intervals, assuming an overall uncertainty of  $\pm 20\%$ . In the source report uncertainties for specific data points were not reported; but a range of  $\pm 15\text{--}20\%$  was estimated by the authors.

Table 6. Neutron flux as measured on AIR-2 flights and as calculated using four different transport option combinations available in CARI-7A<sup>(53, 61, 62) a,b</sup>

Latitude, degrees	Longitude, degrees	Flight date 1997	Depth, g cm <sup>-2</sup>	$R_{VC}$ , GV	$\phi_{\text{meas}}$ , cm <sup>-2</sup> s	$\phi_1$ , cm <sup>-2</sup> s	$\phi_B$ , cm <sup>-2</sup> s	$\phi_{B,S}$ , cm <sup>-2</sup> s	$\phi_{B,A}$ , cm <sup>-2</sup> s
53.9	-117.2	13 Jun	56	0.84	9.88	9.69	10.1	9.74	8.74
18.5	-127.2	11 Jun	53.5	11.76	1.24	1.48	1.43	1.41	1.38
55.6	-120.6	13 Jun	101	0.75	9.64	9.58	10.1	9.38	9.23
37.6	-122.3	8,11,16 Jun	201	4.46	3.39	3.79	3.86	3.37	2.18

<sup>a</sup>The 95% confidence levels for the measurements are  $\pm 8$ ,  $\pm 8$ ,  $\pm 13$ , and  $\pm 16\%$ .

<sup>b</sup>The fluxes were calculated as follows:  $\phi_1$ , using the ISO GCR model and the standard transport options (use nuclear data without angular dependencies for cutoff rigidity or depth);  $\phi_B$ , as  $\phi_1$ , but using the BO11 GCR;  $\phi_{B,S}$ , as  $\phi_B$ , but using the superposition approximation; and  $\phi_{B,A}$ , as  $\phi_B$ , but with all angle-dependent options.

levels [FL] 310, 350 and 390 [flight level is the aviation industry standard for reporting altitudes and is equivalent to feet in hundreds, thus, FL 300 is equivalent to an altitude of about 9 km or an atmospheric depth of  $306 \text{ g cm}^{-2}$ ]<sup>(8)</sup>. It is intended to be used as verification data for more routine methods of dose assessment (i.e. models). The set was derived from over 20 000 measurements made from 1992 to 2006, using a variety of instruments, and analyzed with the Bayesian analysis methods used to create the flight dose calculation computer software FDOScalc<sup>(7)</sup>. ICRU considers models suitable for aviation dosimetry if results are consistently within 30% of the standard data. Figure 2 shows per cent deviations of CARI-7A calculations (using the BO11 GCR model and nuclear transport for HZEs) of  $H^*(10)$  relative to the ICRU data. Agreement is again excellent, with the per cent difference varying from  $-4$  to  $14\%$ , with means and medians at each altitude close to  $5\%$ .

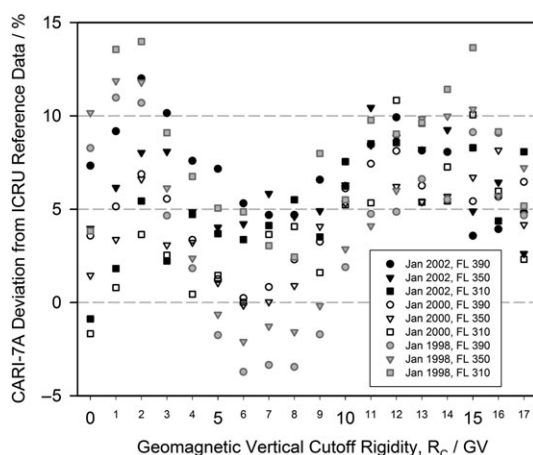


Figure 2. Per cent deviation of calculations from the ICRU reference data set<sup>(8)</sup>. Model calculations used BO11 GCR, angle-independent rigidities and depths, and nuclear transport.

Tables 8–10 show comparisons of calculations (again using the BO11 GCR model and nuclear transport for HZEs) with TEPC measurements. The TEPC data in Tables 8 and 9 is from DLR flights from Fairbanks, AK, US to Frankfurt, Germany on 23 May 2008 and from Dusseldorf, Germany to Mauritius (an island nation in the southern Indian Ocean) on 13–14 February 2008, respectively, as reported by Mertens *et al.*<sup>(17)</sup>. In all,  $H^*(10)$  dose rates around 14 locations during these flights are averaged such that comparable calculations can be made with CARI-7A. For the 14 measurements CARI-7A deviates by an average of  $+5\%$ , consistent with the comparison to the ICRU data set. In Table 10 TEPC data are flight dose measurements of  $H^*(10)$  on flights reported by Lewis *et al.*<sup>(65)</sup>. Again the average deviation is  $+5\%$ , with the calculated flight totals within the relative uncertainty of  $18\%$  reported for the measured doses on 12 of the 13 flights. The notable exception is the trans-equatorial route, for which the dose equivalent is overestimated by  $34\%$ .

## Comparisons with Models

### High altitudes

Figure 3 shows the effective dose profile as calculated by CARI-7A (BO11 GCR model) with and without using superposition, EXPACS v3.00 (based on PHITS), NAIRAS (based on HZETRN), and a special variant of CARI-6 (based on LUIN2000) modified to remove the altitude restriction and calculate effective dose as recommended in ICRP Pub. 103<sup>(13, 17, 18, 66, 67)</sup>. In the calculations done for the figure with EXPACS, which uses the ISO GCR model but with different solar modulation, fluence to effective dose coefficients are taken from ICRP Publications 116 and 123, except for when energies went out of the ICRP range<sup>(68, 69)</sup>. In these cases coefficients are those calculated by Sato *et al.*<sup>(46, 47)</sup>. The coefficient set used was thus almost identical to those used by CARI-6W and CARI-7A. In NAIRAS, the BO11 GCR model is used, but

Table 8. Comparison with DLR in-flight TEPC measurements on a flight from Fairbanks, AK, US to Frankfurt, Germany on 23 May 2008<sup>(17)</sup>.

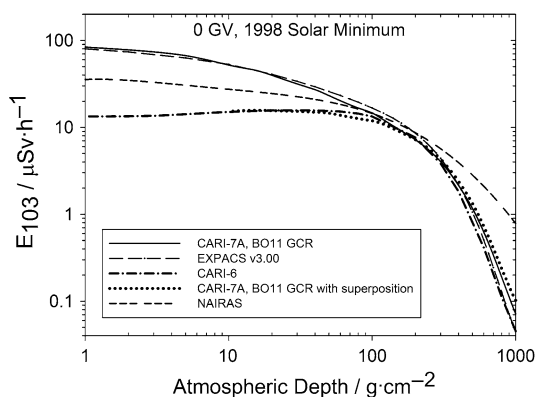
Elapsed flight time, h	Vertical cutoff rigidity, GV	Flight level	CARI-7A $H^*(10)$ , $\mu\text{Sv h}^{-1}$	TEPC $H^*(10)$ , $\mu\text{Sv h}^{-1}$	CARI-7A % deviation from TEPC
1.5	0.1	330	6.00	$5.6(\pm 0.5)$	7.1
2.6	0.0	330	6.00	$6.5(\pm 0.5)$	$-7.7$
3.7	0.0	330	6.00	$5.8(\pm 0.5)$	3.4
5.5	0.1	350	6.89	$6.4(\pm 0.5)$	7.7
6.6	0.4	350	6.89	$5.5(\pm 0.5)$	25
7.4	1.0	350	6.89	$6.2(\pm 0.6)$	11
8.2	1.9	370	7.29	$6.3(\pm 0.5)$	16

**Table 9. Comparison with DLR in-flight TEPC measurements on a flight from Dusseldorf, Germany to Mauritius on 13–14 February 2008<sup>(47)</sup>.**

Elapsed flight time, h	Vertical cutoff rigidity, GV	Flight level	CARI-7A $H^*(10)$ , $\mu\text{Sv h}^{-1}$	TEPC $H^*(10)$ , $\mu\text{Sv h}^{-1}$	CARI-7A % deviation from TEPC
1.0	4.8	350	4.52	4.7( $\pm 0.4$ )	−3.8
2.0	7.2	370	3.80	4.3( $\pm 0.5$ )	−12
2.6	9.3	370	3.18	3.2( $\pm 0.3$ )	−0.62
3.5	12.3	370	2.61	2.9( $\pm 0.2$ )	−9.7
5.0	15.0	370	2.26	2.0( $\pm 0.1$ )	13
7.0	16.0	370	2.15	2.0( $\pm 0.1$ )	7.5
9.5	13.3	410	2.86	2.4( $\pm 0.2$ )	17

**Table 10. Comparison of  $H^*(10)$  calculated flight doses with TEPC measurements of flight doses from Lewis, *et al.*<sup>(65)</sup>.**

City pair <sup>a</sup>	Flight date	CARI-7A $H^*(10)$ , $\mu\text{Sv h}^{-1}$	Measured $H^*(10)$ <sup>b</sup> , $\mu\text{Sv h}^{-1}$	CARI-7A % deviation from measurement
Port Hardy–London, UK	2001/02/27	28.5	28.0	1.79
London, UK–Zagreb, Croatia	2001/02/28	6.24	7.22	−13.6
Zagreb, Croatia–Trenton	2001/03/01	34.1	33.9	0.59
Ottawa–Iqaluit	2001/03/28	9.57	9.32	2.68
Iqaluit–Resolute Bay	2001/03/28	4.56	4.30	6.05
Resolute Bay–Iqaluit	2001/03/28	5.06	4.67	8.35
Iqaluit–Ottawa	2001/03/29	9.68	8.69	11.4
Trenton–Bagotville	2001/05/24	2.93	2.67	9.47
Bagotville–Cold Lake	2001/05/24	14.1	12.4	13.7
Cold Lake–Trenton	2001/05/24	15.1	15.5	2.58
New York, NY, USA–Miami, FL, USA	2001/06/04	10.3	11.0	−6.36
Miami, FL, USA–Buenos Aries, Argentina	2001/06/05	21.1	15.7	34.3
Buenos Aries, Argentina–Auckland, NZ	2001/06/06	54.0	55.8	−3.23

<sup>a</sup>Cities are Canadian unless otherwise noted.<sup>b</sup>Lewis *et al.* estimate 18% relative error for these TEPC data: estimates for individual flights not given.**Figure 3.** ICRP Pub. 103 effective dose rate versus atmospheric depth as calculated at by: CARI-7A using BO11 GCR, angle-independent rigidities and depths, and nuclear transport; EXPACS; CARI-6, which uses superposition; CARI-7A as before but using superposition instead of nuclear transport; and NAIRAS.

fluence-to-dose conversion coefficients are calculated differently. For neutrons and protons the coefficients are used directly, while for heavier particles the coefficients are scaled to the proton coefficients by  $(Z_{\text{eff}})^2/A$ , where  $Z_{\text{eff}}$  is the effective charge, which takes into account the electron capture by HZE particles at low energies. Also, muons and pions are not transported in NAIRAS. The match of CARI-7A with NAIRAS and EXPACS, the other two models with nuclear transport, is quite good at commercial altitudes. All three calculations are in reasonable agreement ( $\pm 30\%$ ) at altitudes between 40 and 300  $\text{g cm}^{-2}$  but NAIRAS drifts away at the highest and lowest altitudes. Regarding the superposition approximation, agreement between CARI-6 (based on LUIN) and the CARI-7A calculation using superposition significantly deviate from the rest of the group as altitude increases, with CARI-7A drifting away from CARI-6 at the lowest altitudes<sup>(13)</sup>. As expected, CARI-7A run using and EXPACS agree very well at the highest

**Table 11. Dose rates at FL 350 calculated by several models for solar minimum conditions at magnetic vertical cutoff rigidities of 0, 5, 10 and 15 GV<sup>(8, 9, 17)</sup>.**

Model	Ambient dose equivalent $H^*(10)$ , $\mu\text{Sv h}^{-1}$			
	0 GV	5 GV	10 GV	15 GV
CARI-7A <sup>a</sup>	6.5	4.4	2.8	2.1
EURADOS <sup>b</sup>	7.0	5	3	1.6
ICRU Ref data <sup>c</sup>	5.9	4.4	2.7	1.9
NAIRAS	4.7	2.8	1.4	0.8

<sup>a</sup>Calculated with BO11, using angle-independent cutoff rigidities and nuclear transport.

<sup>b</sup>Median of 11 codes<sup>(9)</sup>. At 5 GV and 10 GV data are for FL 370 and are thus overestimates.

<sup>c</sup>Methods used by Wissmann *et al.* to create FDOScale applied to an expanded set of measurements<sup>(7, 8)</sup>.

altitudes, before transport methods play a significant role. The influence of fluence to dose coefficients choice is evident from the large difference between NAIRAS and CARI-7A (and EXPACS). Considering the differences in transport codes and dose calculation techniques, the results show surprisingly good agreement at the most common commercial flight altitudes.

#### Commercial flight altitudes

The 2012 EURADOS report contains extensive comparisons of several modern models (AVIDOS, CARI-6, EPCARD.Net, FDOSCalc, IASON-FREE, JISCARD EX, PANDOCA, PCAIRE, PLANETOCOSMICS [Bern model], QARM and SIEVERT), but doses are reported in an anonymous manner to avoid to endorsing any one model more favorably than any of the others<sup>(9)</sup>. Table 11 shows calculated dose rates at flight level 350 during solar minimum conditions at locations with magnetic vertical cutoff rigidities of 0, 5, 10 and 15 GV. In addition to CARI-7A calculations (using the BO11 GCR model, angular cutoffs, depth related corrections and nuclear transport for HZEs) and the median calculation reported by EURADOS, the table contains NAIRAS calculations (not available when the EURADOS report was assembled), and ICRU Rep. 84 reference data, which provides an independent benchmark for all the models<sup>(8, 17)</sup>.

#### DISCUSSION

All comparisons with measurements are consistent in terms of trends. With respect to dose rates, there is as an upward trend relative to measurements in the calculated dose rates as depth increases, which for  $H^*(10)$  is about 5% high at commercial altitudes,

and somewhat lower relative to the ER-2 measurements. Since the dose equivalent data are mostly TEPC data, the differences between TEPC dose equivalent conversion to  $H^*(10)$  and theoretical  $H^*(10)$  may play some role. Also, in the case of the HARES data, some difference is certainly the result of comparing different quantities: calculated whole-body-averaged absorbed dose and measured TEPC absorbed dose. The trend when comparing neutron flux with the Bonner sphere data are similar to trends when comparing calculations to the TEPC dose equivalent, but the neutron data are sparse.

There is also an interesting periodicity relative to cutoff at all three altitudes of the ICRU data. The reason for this trend is unknown.

Despite all the shortcomings, comparisons of the CARI-7A model dose rates and flight doses with measurements and other models are excellent at all altitudes currently important to aviation.

CARI-7A is superior to CARI-6 for those seeking to calculate  $H^*(10)$  or  $E_{103}$ , as there is no provision in most CARI-6 releases for calculating those kinds of doses (conversion factors could be used, of course) or doses at altitudes above FL 600. For those calculating  $E_{60}$  at commercial flight altitudes, there is little to be gained by moving to CARI-7A from CARI-6, except that CARI-7A can run without a DOS emulator on modern operating systems, as it is built in a more cross-platform compatible manner.

In regards to future developments in CARI-7A, GCR model choices will be expanded with more recent models such as that of Mathiä *et al.*, the newer Badwhar and O'Neill 2014 model, and any update to the ISO standard model (which was examined for possible update in 2013, but left unchanged)<sup>(20, 70–72)</sup>. Solar particle event spectra are also being considered. As reported by Sato, as simple slant function, while shown to be within a factor of two here for dose calculations at most altitudes, can be improved<sup>(73)</sup>. Other developments currently underway in CARI-7A include: conversion to use of official ICRP  $E_{103}$  coefficients where possible, optimization of interpolation and numerical integration methods to best match table data shapes, allowance for incorporation of thin shields of vehicle structure materials (besides equivalent atmospheric depth) in the calculations, to improve accuracy for flights at the edge of space and for commercial space flights spending significant time in a few grams per centimeter square of atmosphere or less; and expanding output options to include particle spectra. Also, a less scientifically oriented and faster running version of CARI-7 derived from CARI-7A, similar to CARI-6 in simplicity of upkeep and output, is planned for release as soon as it is ready.

The aviation community would benefit from more complete sets of fluence-to-dose conversion coefficients using isotropic-from-above exposure, including

coefficients for *HZE* particles. Also, another useful study would be an evaluation of the influence of aircraft structure on the dose rate to occupants as related to altitude and vehicle size and primary structural materials. This would establish, more definitively, altitudes above which vehicle structure (traditionally ignored for calculations of doses to aircraft occupants, but not for spacecraft occupants) of lightly shielding vehicles should be accounted for in some way when calculating doses to vehicle occupants. Of course, for such high altitude vehicles, designers are likely to use a less general approach to radiation exposure analysis.

## FUNDING

This work was supported by the Aerospace Medical Research Division of the Civil Aerospace Medical Institute (CAMI) operated by the United States Department of Transportation Federal Aviation Administration Office of Aerospace Medicine.

## ACKNOWLEDGMENTS

The author thanks: the CAMI librarians, Roni Anderson and Kathy Wade, for help obtaining references; the CAMI editor (ret.), Mike Wayda, for proofreading the manuscript; Maurizio Pelliccioni for providing his organ dose data; Tatsuhiko Sato for providing EXPACS results and his comments on the manuscript; Chris Mertens for providing NAIRAS data and BO11 data; Mike James, Greg McKinney and Forrest Brown for answering questions about MCNP and MCNPX; Brent Lewis, Emily Corcoran, Francois Lemay, Hughes Bonin, and Kristine Spekkens for their comments on reference 12 leading to some of the improvements in CARI shown here; and Paul Goldhagen for providing his latest evaluation of the AIR-2 neutron flux data, comments on the manuscript and hours of enlightening discussions.

## REFERENCES

1. United Nations Scientific Committee on the Effects of Atomic Radiation (UNSCEAR). Sources and effects of ionizing radiation: United Nations Scientific Committee on the Effects of Atomic Radiation: UNSCEAR 2000 report to the General Assembly, with scientific annexes, Volume I: Sources (New York, NY: United Nations) (2000).
2. Cucinotta, F. A. *et al.* Space radiation and cataracts in astronauts. *Radiat. Res.* **156**, 460–466 (2001).
3. Grajewski, B. *et al.* Miscarriage among flight attendants. *Epidemiology* **26**(2), 192–203 (2015) 10.1097/EDE.0000000000000225.
4. National Council on Radiation Protection and Measurements (NCRP) 2006. Information needed to make radioprotection recommendations for space missions beyond low-Earth orbit. NCRP Report No. 153, (Bethesda, MD: NCRP).
5. Lewis, B. J. *et al.* Assessment of aircrew radiation exposure by further measurements and model development. *Radiat. Prot. Dosim.* **111**(2), 151–171 (2004).
6. McCall, M. J., Lemay, F., Bean, M. R., Lewis, B. J. and Bennett, L. G. Development of a predictive code for aircrew radiation exposure. *Radiat. Prot. Dosim.* **136**(4), 274–81 (2009) 10.1093/rpd/ncp130.
7. Wissmann, F., Reginatto, M. and Möller, T. Ambient dose equivalent at flight altitudes: a fit to a large set of data using a Bayesian approach. *J. Radiol. Prot.* **30**, 513–524 (2010).
8. International Commission on Radiation Units and Measurements (ICRU). Reference data for the validation of doses from cosmic-radiation exposure of aircraft crew. ICRU Report 84, J. ICRU, **10**(2). (Oxford, UK: Oxford University Press (2010)).
9. Bottollier-Depois, J. F. *et al.* Comparison of codes assessing radiation exposure of aircraft crew due to galactic cosmic radiation. EURADOS Report 2012-03 (Braunschweig, Germany: European Radiation Dosimetry Group e.V) (2012).
10. Wall, M. For sale: Balloon rides to near-space for \$75,000 a seat. by SPACE.COM (October 22, 2013 issue) available at [www.space.com/23291-space-tourism-balloon-flights.html](http://www.space.com/23291-space-tourism-balloon-flights.html). (13 December 2016, date last accessed)
11. Lei, F., Hands, A., Truscott, P. and Dyer, C. Cosmic-ray heavy ions contributions to the atmospheric radiation field. In: 2009 European Conference on Radiation and its Effects on Components and Systems (RADECS), pp. 375–376 (2009), doi: 10.1109/RADECS.2009.5994679.
12. Copeland, K. Cosmic ray particle fluences in the atmosphere resulting from primary cosmic ray heavy ions and their resulting effects on dose rates to aircraft occupants as calculated with MCNPX 2.7.0. Doctoral Thesis, Royal Military College of Canada, Kingston, Ontario, Canada) (2014).
13. O'Brien, K. *et al.* World-wide radiation dosage calculations for air crew members. *Adv. Space Res.* **31**(4), 835–840 (2003).
14. Copeland, K., Sauer, H. H., Duke, F. E. and Friedberg, W. Cosmic radiation exposure of aircraft occupants on simulated high-latitude flights during solar proton events from 1 January 1986 through 1 January 2008. *Adv. Space Res.* **42**(6), 1008–1029 (2008).
15. Pelowitz, D. B. Ed. . *MCNPX User's Manual, Version 2.7.0*. Report LA-CP-11-00438 (Los Alamos, NM: Los Alamos National Laboratory) (2011).
16. Oak Ridge National Laboratory (ORNL). Monte Carlo N-Particle Transport Code System for Multiparticle and High Energy Applications (MCNPX 2.7.0) RSICC code package C740 (2011), developed at Los Alamos National Laboratory (available from the Radiation Safety Information Computational Center at ORNL, Oak Ridge, TN).
17. Mertens, C. J., Meier, M. M., Brown, S., Norman, R. B. and Xu, X. NAIRAS aircraft radiation model development, dose climatology, and initial validation. *Space Weather* **11**, 1–33 (2013) 10.1002/swe.20100.
18. Sato, T. *et al.* Particle and heavy ion transport code system PHITS, Version 2.52. *J. Nucl. Sci. Technol.* **50**(9), 913–923 (2013).

19. Adams, J. H. Jr, Heiblim, S. and Malott, C. *Evaluation of galactic cosmic ray models*, presented at IEEE Nucl Space Radiat Effects Conf, Quebec City, QC, Can, Jul 2009 (2009). Available at: <https://ntrs.nasa.gov/search.jsp?N=0&Ntk=All&Ntt=20090034942&Ntx=mode%20matchallpartial&Nm=1231Collection/NASA%20STII17Collection/NACA>
20. International Standards Organization *Space Environment (Natural and Artificial) – Galactic Cosmic Ray Model* (ISO 15930:2004) (Geneva, Switzerland: ISO) (2004).
21. O'Neill, P. M. *Badhwar–O'Neill 2010 galactic cosmic ray flux model—revised*. IEEE Trans. Nucl. Sci. **57**(6), 3148–3153 (2010) 10.1109/TNS.2010.2083688.
22. Lantos, P. *Forbush decrease effects on radiation dose received on-board aeroplanes*. Radiat. Prot. Dosim. **117** (4), 357–64 (2005).
23. Mewaldt, R. A. *Elemental composition and energy of galactic cosmic rays*. In: Proceedings of Workshop on the Interplanetary Charged Particle Environment, Jet Propulsion Laboratory, Pasadena, CA), pp. 121–132 (1988).
24. O'Brien, K. Personal Communication to Wallace Friedberg. A 1×1 Degree World Grid of interpolated Cosmic Ray Vertical Cutoff Rigidities from IGRF 1995, based on a 5×15 degree table calculated by D.F. Smart and M.A. Shea (1999).
25. Shea, M. A., Smart, D. F. and McCall, J. R. *A five degree by fifteen degree world grid of trajectory determined vertical cutoff rigidities*. Can. J. Phys. **46**, S1028–S1101 (1968).
26. Shea, M. A. and Smart, D. F. *A world grid of calculated cosmic ray vertical cutoff rigidities for 1980.0*. In: 18th International Cosmic Ray Conference, Conference Papers, 3, p. 415 (1983).
27. Smart, D. F. and Shea, M. A. *World grid of calculated cosmic ray vertical cutoff rigidities for epoch 1990*. In: 25th International Cosmic Ray Conference, Conference Papers, 2, pp. 401–404 (1997).
28. Smart, D. F. *Vertical Geomagnetic Cutoff Rigidity Latitude Plots: IGRF 2000*. Report for FAA CAMI contract AC-04-02566 (2005).
29. Smart, D. F. and Shea, M. A. *World grid of calculated cosmic ray vertical cutoff rigidities from IGRF 2010*, in partial fulfillment of FAA Procurement AAM-610-12-0157 (2012).
30. Al Anid, H., Lewis, B. J., Bennett, L. G. I. and Takada, M. *Modelling of solar radiation exposure at high altitude during solar storms*. Radiat. Prot. Dosim. **136**(4), 311–316 (2009) 10.1093/rpd/ncp127.
31. Clem, J. M. *et al.* *Contribution of obliquely incident particles to neutron monitor counting rate*. J. Geophys. Res. **102**(A12), 26919–26926 (1997).
32. Ferrari, A., Sala, P. R., Fasso, A. and Ranft, J. *FLUKA: a multi-particle transport code* CERN-2005-10, INFN/TC\_05/11, SLAC-R-773 (2005).
33. Dorman, L. I. *et al.* *Effective non-vertical and apparent cutoff rigidities for a cosmic ray latitude survey from Antarctica to Italy in minimum of solar activity*. Adv. Space Res. **42**(3), 510–516 (2008).
34. Smart, D. F. and Shea, M. A. *The limitations of using vertical cutoff rigidities determined from the IGRF magnetic field models for computing aircraft radiation dose*. Adv. Space Res. **32**(1), 95–102 (2003) 10.1016/S0273-1177(03)00501-5.
35. Störmer, C. *The Polar Aurora* (London: Oxford University Press) (1950).
36. National Oceanic and Atmospheric Administration (NOAA), National Aeronautics and Space Administration, and United States Air Force *U.S. Standard Atmosphere, 1976* (NOAA-S/T 76-1562) (Washington, DC: NOAA) (1976).
37. International Commission on Radiation Units and Measurements (ICRU). *Stopping powers and ranges for protons and alpha particles*. ICRU Report 49. (Bethesda, MD: International Commission on Radiation Units and Measurements, Inc) (1993).
38. James, M. and McKinney, G. Private communications, 2012 (2012).
39. Huestis, D. L. *Accurate evaluation of the Chapman function for atmospheric attenuation*. J. Quant. Spectrosc. Radiat. Transfer **69**(6), 709–721 (2001) 10.1016/S0022-4073(00)00107-2.
40. McMath, G. E. and McKinney, G. W. *MCNP6 elevation scaling of cosmic ray backgrounds*. Report LA-UR-14-21331 (Los Alamos, NM: Los Alamos National Laboratory) (2014).
41. International Commission on Radiological Protection (ICRP). *1990 recommendations of the International Commission on Radiological Protection*. ICRP Pub 60 (Tarrytown, NY: Elsevier Science) (1991).
42. International Commission on Radiological Protection (ICRP). *The 2007 recommendations of the International Commission on Radiological Protection*. ICRP Pub 103 (London, UK: Elsevier) (2007).
43. International Commission on Radiation Units and Measurements (ICRU). *Quantities and Units in Radiation Protection Dosimetry*. ICRU Report 51 (Bethesda, MD: ICRU Publications) (1993).
44. Ferrari, A. and Pelliccioni, M. *On the conversion coefficients for cosmic ray dosimetry*. Radiat. Prot. Dosim. **104**(3), 211–220 (2003).
45. Pelliccioni, M. *Overview of fluence-to-effective dose and fluence-to-ambient dose equivalent conversion coefficients for high energy radiation calculated using FLUKA code*. Radiat. Prot. Dosim. **88**(4), 279–297 (2000).
46. Sato, T., Endo, A., Zankl, M., Petoussi-Henss, N. and Niita, K. *Fluence-to-dose conversion coefficients for neutrons and protons calculated using the PHITS code and ICRU/ICRP adult reference computational phantoms*. Phys. Med. Biol. **54**, 1997–2014 (2009) 10.1088/0031-9155/54/7/009.
47. Sato, T., Endo, A. and Niita, K. *Fluence-to-dose conversion coefficients for heavy ions calculated using the PHITS code and the ICRP/ICRU adult reference computational phantoms*. Phys. Med. Biol. **55**, 2235 (2010) 10.1088/0031-9155/55/8/008.
48. Sato, T., Tsuda, S., Sakamoto, Y., Yamaguchi, Y. and Niita, K. *Conversion coefficients from fluence to effective dose for heavy ions with energies up to 3 GeV/A*. Radiat. Prot. Dosim. **106**(2), 137–144 (2003).
49. Niita, K. *et al.* *Computer Program PHITS: Particle and Heavy Ion Transport code System, Version 2.23*. JAEA-Data/Code 2010-022 (2010).
50. Pelliccioni, M. Private communication of organ dose data for reference 38 (14 April 2005).
51. Copeland, K., Friedberg, W., Sato, T. and Niita, K. *Comparison of fluence-to-dose conversion coefficients for deuterons, tritons, and helions*. Radiat. Prot. Dosim. **148**(3), 344–351 (2012) 10.1093/rpd/ncr035.

52. Frakes, S. J. Computer programs INVERSE and FORWARD (2002). Available at: [http://www.ngs.noaa.gov/PC\\_PROD/Inv\\_Fwd/](http://www.ngs.noaa.gov/PC_PROD/Inv_Fwd/) (accessed June 29, 2012).
53. Goldhagen, P. Private communication, July 25, 2014 (2014). Revised data for neutron spectra and total neutron fluxes measured on the ER-2 aircraft at 4 locations.
54. Battistoni, G., Ferrari, A., Pelliccioni, M. and Villari, R. *Evaluation of the doses to aircrew members taking into consideration the aircraft structures*. Adv. Space Res. **36**, 1645–1652 (2005).
55. Foelsche, T., Mendell, R. B., Wilson, J. W. and Adams, R. R. Measured and calculated neutron spectra and dose equivalent rates at high altitudes; relevance to SST operations and space research. Report No. NASA TN D-7715 (Washington, DC: National Aeronautics and Space Administration) (1974).
56. Various. MCNP Reference Collection. Available at [https://laws.lanl.gov/vhosts/mcnp.lanl.gov/references.shtml#mcnpx\\_refs](https://laws.lanl.gov/vhosts/mcnp.lanl.gov/references.shtml#mcnpx_refs) (last date accessed September 19, 2016).
57. Felsberger, E., O'Brien, K. and Kindl, P. *IASON-FREE: theory and experimental comparisons*. Radiat. Prot. Dosim. **136**(4), 267–273 (2009) 10.1093/rpd/ncp128.
58. Copeland, K. *Influence of the superposition approximation on calculated effective dose rates from galactic cosmic rays at aerospace related altitudes*. Space Weather **13**(7), 401–405 (2015) 10.1002/2015SW001210.
59. Goldhagen, P. *Overview of aircraft radiation exposure and recent ER-2 measurements*. Health Phys. **79**(5), 526–544 (2000).
60. Wilson, J. W., et al. *Summary of atmospheric ionizing AIR research: SST-Present*. In Wilson, J. W. Jones, I. W., Maiden, D. L., Goldhagen, P. Eds. *Atmospheric Ionizing Radiation (AIR): Analysis, results, and lessons learned from the June 1997 ER-2 campaign*, Proceedings of a workshop, Langley Research Center, Hampton, VA, March 30–31, 1998. Report NASA/CP-2003-212155, Chapter 21, pp. 387–407 (2003).
61. Goldhagen, P., Clem, J. M. and Wilson, J. W. *The energy spectrum of cosmic-ray induced neutrons measured on an airplane over a wide range of altitude and latitude*. Radiat. Prot. Dosim. **110**, 387–392 (2004).
62. Goldhagen, P. Private communication, Oct. 4, 2016 (2016). Revised uncertainty estimates for total neutron fluxes measured on the ER-2 aircraft at 4 locations.
63. Advisory Committee for Radiobiology Aspects of the SST. *ARCBASST final report: cosmic radiation exposure in supersonic and subsonic flight*. Aviat. Space Environ. Med. **46**(9), 1170–1185 (1975).
64. Kuehner, A. V., Chester, J. D. and Baum, J. W. *Portable mixed radiation dose equivalent meter*. Report No. BNL 17298 (Upton, NY, USA: Brookhaven National Laboratory) (1972).
65. Lewis, B. J. et al. *Galactic and solar radiation exposure to aircrew during a solar cycle*. Radiat. Prot. Dosim. **102**(3), 207–227 (2002).
66. Copeland, K. *Recent and planned developments in the CARI program*. Federal Aviation Administration Office of Aviation Medicine Report, DOT/FAA/AM-13/6 (2013).
67. Sato, T. *Analytical model for estimating terrestrial cosmic ray fluxes nearly anytime and anywhere in the world: extension of PARMA/EXPACS*. PLOS One **10** (12), e0144679 (2015).
68. International Commission on Radiological Protection. *Conversion coefficients for radiological protection quantities for external radiation exposures*. ICRP Publication 116. Ann. ICRP **40**(2–5) (London, UK: Elsevier (2010).
69. International Commission on Radiological Protection (ICRP). *Assessment of radiation exposure of astronauts in space*. ICRP Publication 123 (London, UK: Elsevier) (2013).
70. Mathiä, D., Berger, T., Mrigakshi, A. I. and Reitz, G. *A ready-to-use galactic cosmic ray model*. Adv Space Res. **51**, 329–338 (2013) 10.1016/j.asr.2012.09.022.
71. O'Neill, P. M., Golge, S. and Slaba, T. C. and Badhwar – O'Neill 2014 Galactic Cosmic Ray Flux Model Description. Report No. NASA/TP–2015–218569. Houston, TX, USA: National Aeronautics and Space Administration Johnson Space Center (2015). Available at: [ntrs.nasa.gov/search.jsp?R=20150003026](https://ntrs.nasa.gov/search.jsp?R=20150003026) (accessed May 5, 2016).
72. International Standards Organization (ISO). Official Webpage for standard ISO 15390:2004: [http://www.iso.org/iso/iso\\_catalogue/catalogue\\_tc/catalogue\\_detail.htm?csnumber=37095](http://www.iso.org/iso/iso_catalogue/catalogue_tc/catalogue_detail.htm?csnumber=37095) (accessed September 19, 2016).
73. Sato, T. *Analytical model for estimating the zenith angle dependence of terrestrial cosmic ray fluxes*. PLOS One **11**(8), e0160390 doi:10.1371/journal.pone.0160390.